Cement & Concrete Composites 43 (2013) 31–38

Contents lists available at SciVerse ScienceDirect

Cement & Concrete Composites

journal homepage: www.elsevier.com/locate/cemconcomp

Comparative study of three sodium phosphates as corrosion inhibitors for steel reinforcements

D.M. Bastidas [a], M. Criado [a], V.M. La Iglesia [a], S. Fajardo [a], A. La Iglesia [b], J.M. Bastidas [a,*]

[a] National Centre for Metallurgical Research (CENIM), CSIC, Avda. Gregorio del Amo 8, 28040 Madrid, Spain
[b] Institute of Geosciences, CSIC, UCM, C/. Jose Antonio Novais 2, 28040 Madrid, Spain

ARTICLE INFO

Article history:
Received 11 January 2012
Received in revised form 10 June 2013
Accepted 12 June 2013
Available online 21 June 2013

Keywords:
Steel-reinforced cement mortar
OPC paste
Phosphates
Diffusion
Migrating corrosion inhibitor
Admixture corrosion inhibitor

ABSTRACT

A comparative study was performed on the inhibition of steel reinforcement corrosion using three soluble phosphates: sodium monofluorophosphate (Na_2PO_3F), disodium hydrogen phosphate (Na_2HPO_4) and trisodium phosphate (Na_3PO_4). Tests were carried out using ordinary Portland cement (OPC) paste specimens and OPC mortar specimens with embedded steel reinforcements. The corrosion inhibitors were deployed in two different ways: by immersion of OPC specimens in aqueous solutions containing the soluble phosphates (migrating corrosion inhibitor), and by addition of the phosphate powders to a fresh OPC paste (admixture corrosion inhibitor). After curing, the tested specimens were studied using X-ray diffraction, wavelength-dispersive electron microprobe analysis, linear polarisation resistance and electrochemical corrosion potential. A correlation was found between the phosphate content (by migration or admixture) in the OPC matrices and the steel corrosion rate.

1. Introduction

Many different methods have been proposed to address rebar corrosion in reinforced concrete structures, such as barrier layers, cathodic protection and corrosion inhibitors. Corrosion inhibitors may be a good way to prevent and/or control reinforcing steel corrosion because they are easy to apply and less costly than other prevention methods [1,2].

Corrosion inhibitors may be classified according to their application procedure, protection mechanism or composition [3]. They can be deployed by addition to the fresh cement paste, as an admixture corrosion inhibitor, or by application on the hardened concrete surface, as a penetrating or migrating corrosion inhibitor [4]. The latter inhibitors are transmitted through the concrete to the reinforcements by means of a diffusion process.

Alternatively, steel rebars can be treated with a phosphate solution to coat the metal surface with an integrated, mildly protective insoluble crystal layer [5–7]. In the phosphating process, iron dissolution takes place at the substrate microanodes and hydrogen is evolved at the microcathodes [8–10]:

$$Fe + 2H_3PO_4 \leftrightarrows Fe(H_2PO_4)_2 + H_2 \quad (1)$$

The formation of a soluble ferrous phosphate leads to a decrease in the phosphoric acid concentration, and as a result an increase in the pH at the metal/solution interface. This change in pH alters the hydrolytic equilibrium between the soluble primary phosphates and the insoluble tertiary phosphates of the iron present in the phosphating solution, resulting in the rapid conversion and deposition of insoluble tertiary iron phosphate [11].

Phosphating processes help to protect steel against corrosion and provide a good anchoring capability. The barrier performance of the phosphate layer depends on its insulating ability and porosity [12]. In recent work, Manna studied the effect of a phosphate coating on steel substrates with different thermomechanical treatments [13,14]. The best results in terms of corrosion behaviour and bond strength were recorded for tempered martensitic steel. The effectiveness of a Zn–Ca phosphate system has also been reported [15], showing a 74% enhancement in the bond strength between the rebar and the concrete. Minimum corrosion current and maximum corrosion potential values were obtained for the Zn–Ni phosphate conversion coating system, showing its optimum corrosion resistance.

The use of phosphate compounds as corrosion inhibitors has been widely studied, but there continues to be a lack of consensus about the inhibition mechanism, which can be anodic, cathodic or mixed [16,17]. Phosphates offer an environmentally friendly alternative to traditional sodium nitrite ($NaNO_2$) inhibitors [18,19].

Soluble phosphates, traditionally disodium hydrogen phosphate (DHP), or sodium monofluorophosphate (MFP), can be deployed in concrete in two ways: by mixing with the cement, sand and water as an admixture corrosion inhibitor [18,20], or by immersion of the concrete in a phosphate solution or surface application of a phosphate solution by brushing as a migrating corrosion inhibitor

* Corresponding author. Tel.: +34 91 553 8900; fax: +34 91 534 7425.
E-mail address: bastidas@cenim.csic.es (J.M. Bastidas).

0958-9465/$ - see front matter © 2013 Elsevier Ltd. All rights reserved.
http://dx.doi.org/10.1016/j.cemconcomp.2013.06.005

[21]. With the latter methods, phosphates penetrate the concrete pore network by capillarity. In all cases, the soluble phosphates react with calcium hydroxide (portlandite) ($Ca(OH)_2$) to trigger the precipitation of an insoluble calcium phosphate. Some criticisms of this mechanism are that DHP or MFP are thus obstructed from reaching the embedded steel surface, reducing their capacity to act as corrosion inhibitors [22–25].

This paper studies the performance of three soluble phosphates: MFP, DHP and trisodium phosphate (TSP), as corrosion inhibitors for reinforced mortar, and evaluates the effectiveness of their application by addition to a fresh cement paste as an admixture corrosion inhibitor or by diffusion as a migrating corrosion inhibitor through the immersion of mortar specimens in an aqueous MFP, DHP or TSP solution.

2. Experimental programme

Type I 52.5 N/SR ordinary Portland cement (OPC) with the chemical composition given in Table 1 was used. Its particle size distribution (Fig. 1) was obtained by laser ray diffraction and showed only one mode, where 10% of the particles were smaller than 1.5 μm, 50% smaller than 10.5 μm and 90% smaller than 29.2 μm.

Carbon steel bars of 8 mm in diameter and a chemical composition of 0.45% C, 0.22% Si, 0.72% Mn, <0.010% P, 0.022% S, 0.13% Cr, 0.13% Ni, 0.18% Cu and balance Fe were used as reinforcements.

Three soluble phosphate compounds were tested as reinforcing steel corrosion inhibitors: 95% pure Aldrich sodium monofluorophosphate (Na_2PO_3F), 99% pure Panreac disodium hydrogen phosphate (Na_2HPO_4), and 97% pure Panreac trisodium phosphate 1-hydrate (Na_3PO_4).

Two types of specimens were tested: cement paste specimens and mortar specimens with embedded steel reinforcement bars.

Cement paste specimens were made by mixing the OPC with water at a constant water/cement ratio of 0.35. Pastes were prepared with 3% additions of the studied phosphates (MFP, DHP or TSP) and without phosphates. The fresh paste was poured immediately into 10 × 10 × 60 mm moulds and cured in conditions of 100% relative humidity (RH) for 30 days at room temperature.

The cement paste specimens with 3% addition of phosphates were used to study phosphate distribution by wavelength-dispersive electron microprobe analysis (EMPA). A JEOL JXA-8900M unit was used under operating conditions of 20 kV acceleration voltage, 50 nA current, 20 s peak counting time, 5 s background counting time, and a beam diameter of 20 μm. EMPA analysis determines the phosphorus content as P_2O_5.

The cement paste specimens without phosphates were used to perform diffusion experiments by immersion in a 0.2 M aqueous MFP, DHP or TSP solution (migrating corrosion inhibitor specimens), according to the method used by López-Acevedo et al. [26], for a period of 60 days.

Table 1
Chemical compositions (% in mass) of tested ordinary Portland cement (OPC).

Compound	Composition (%)
SiO_2	20.33
Al_2O_3	3.40
Fe_2O_3	4.68
CaO	57.84
MgO	1.51
MnO	0.10
TiO_2	0.09
K_2O	0.72
Na_2O	0.51
SO_3	7.26
Loss on ignition	3.42
Insoluble residue	1.23

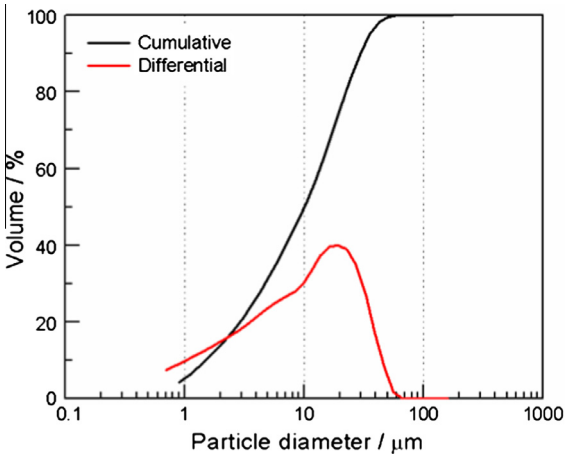

Fig. 1. Granulometry distribution of the tested ordinary Portland cement (OPC) obtained using the laser ray diffraction method.

Cement paste specimen preparation for EMPA analysis consisted of taking 6 mm thick slices with a cross section of 10 × 10 mm from the core of the prism 30 mm from the square base, encapsulation in epoxy resin, and polishing with aluminium oxide powder paste of 0.05 μm grain diameter. Fifty microprobe spots spaced 190 μm apart were analysed along a 10 mm line. All measurements were made on two replicate specimens. Crystalline phases present in the specimens were characterised by X-ray diffraction (XRD) using a Bruker D8 Advance diffractometer with Sol-X detector. X-ray patterns were recorded from 5° to 65° (2θ) in the step-scanning mode, step size 0.02° (2θ), and 1 s counting time.

Mortar specimens of 20 × 55 × 80 mm dimensions were prepared using siliceous sand (SiO_2, 99% pure) with a water/sand/cement ratio of 0.5/3/1. Two 8 mm diameter carbon steel bars were symmetrically embedded lengthwise in the specimens and a stainless steel cylinder of 50 mm in diameter was inserted in a central position. The curing conditions were the same as for the cement paste specimens: 100% RH for 30 days at room temperature, prior to the electrochemical measurements campaign. The mortar specimens without phosphates were immersed in a 0.2 M aqueous MFP, DHP or TSP solution or in distiled water at room temperature (migrating corrosion inhibitor specimens). The mortar specimens with phosphates were stored in desiccators at saturation RH (~100%) at room temperature (admixture corrosion inhibitor specimens).

The mortar specimens were used to carry out electrochemical corrosion tests, with the carbon steel bars acting as working electrodes and the stainless steel cylinder as counter electrode. A central drillhole in the latter allowed the use of a saturated calomel electrode (SCE) as reference. A pad soaked in distiled water was used to facilitate the electrical measurements. An active surface area of 10 cm^2 was marked on the working electrodes with adhesive tape, thus isolating the triple-mortar/steel/atmosphere interface to avoid possible localised corrosion attack due to differential aeration. Corrosion behaviour over time was monitored using the electrochemical corrosion potential (E_{corr}) and linear polarisation resistance (R_p) techniques ($R_p = \Delta E/\Delta I$). This allows the steel corrosion rate (current density) to be calculated using the Stern–Geary equation [27]: $i_{corr} = B/R_p$, where B is a constant determined at the end of the experiment by performing polarisation curves, applying a polarisation of -200 mV < E_{corr} < +200 mV, $B = (\beta_a\beta_c)/2.303(\beta_a + \beta_c)$, β_a and β_c are the anodic and cathodic Tafel

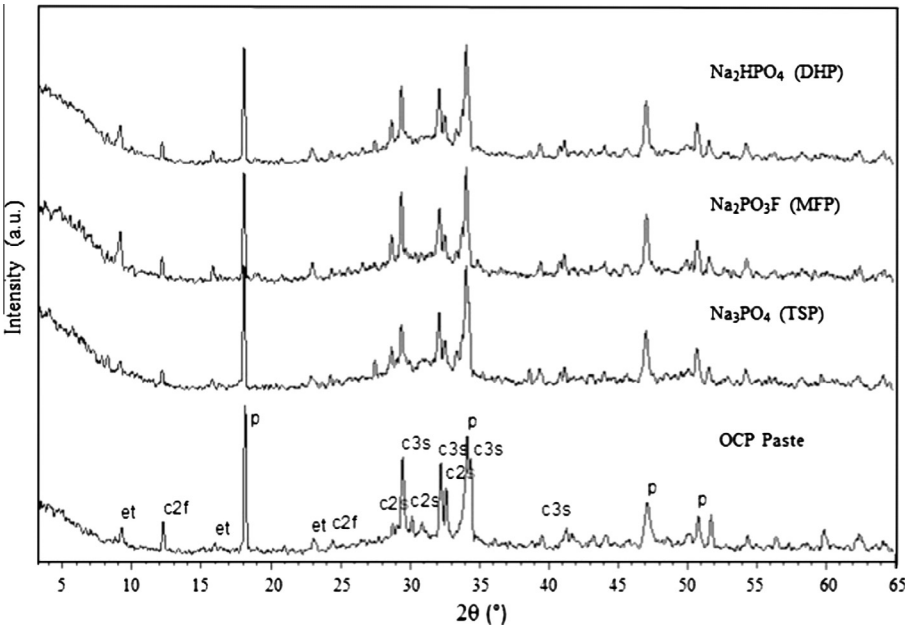

Fig. 2. XRD patterns for admixture corrosion inhibitor specimens. Ordinary Portland cement (OPC) (OPC Paste: blank experiment), OPC mixed with 3% Na_3PO_4 (TSP), OPC mixed with 3% Na_2PO_3F (MFP), and OPC mixed with 3% Na_2HPO_4 (DHP). et: ettringite, c2f: calcium iron oxide, p: portlandite, c2s: calcium silicate (Ca_2SiO_4), c3s: calcium silicate oxide (Ca_3SiO_4O).

slopes, respectively [28]. An EG&G Parc potentiostat model 273A was used for electrochemical measurements.

3. Results

Fig. 2 displays representative XRD patterns for cement paste specimens with admixture corrosion inhibitor cured at 100% RH for 30 days. The patterns show similar behaviour both with and without phosphate, which may indicate that the presence of a small amount of phosphates does not have a significant influence on curing reactions, and at the same time that new crystalline phases were not formed (for the 1–3% detection limit of the XRD technique). XRD patterns (not included) for specimens without phosphate immersed for 60 days (after curing) in 0.2 M aqueous phosphate solutions (MFP, DHP or TSP) also showed no change in relation to the original OPC paste specimen.

Fig. 3 shows the phosphorus distribution (as % P_2O_5) as a function of the penetration depth for migrating corrosion inhibitor specimens using the EMPA technique. As can be observed, after an initial fast decrease the P_2O_5 distribution is homogeneously of the order of ~0.10%. The P_2O_5 penetration depth was determined by the intercept of the tangent associated to the sharp decay curve showing the variation in P_2O_5 versus penetration depth and the abscissa axis. Table 2 summarises the results for P_2O_5 penetration depths. It can be seen that DHP and TSP compounds present similar P_2O_5 penetration values, 380 μm and 126 μm, respectively, while the MFP compound presents the highest penetration depth, 1114 μm.

EMPA results allow the intrinsic phosphate diffusivity to be calculated for the MFP, DHP and TSP corrosion inhibitors in OPC paste. The diffusion coefficient for each phosphate compound may be estimated by analysing the PO_4^{3-} content distribution over the penetration depth based on the one-dimensional solution to Fick's second law of diffusion [29]:

$$\frac{C(x,t)-C_0}{C_S-C_0}=1-\mathrm{erf}\left(\frac{x}{2\sqrt{Dt}}\right) \quad (2)$$

where $C(x,t)$ is the PO_4^{3-} content at penetration depth (x) at time (t); t is the exposure time; x is the depth; C_0 is the initial or background PO_4^{3-} content in the OPC paste; C_S is the PO_4^{3-} content on the exposed surface; D is the effective diffusion coefficient; and erf is the Gaussian error function, ($\mathrm{erf}(x)\equiv\frac{2}{\sqrt{\pi}}\int_0^x e^{-y^2}dy$) [30]. The effective diffusion coefficients (D) obtained using Eq. (2) are listed in Table 2, presenting D values of 1.8×10^{-8} $cm^2\,s^{-1}$ for MFP, 6.7×10^{-9} $cm^2\,s^{-1}$ for DHP, and 5.0×10^{-9} $cm^2\,s^{-1}$ for TSP, thus indicating a decreasing diffusion rate in the order MFP > DHP > TSP. Since the penetration depths of phosphorous are small, the diffusion coefficient values should be regarded as approximations.

Fig. 4 shows the phosphorus distribution (as % P_2O_5) versus depth for admixture corrosion inhibitor specimens using the EMPA technique. As can be observed, the P_2O_5 distribution is inhomogeneous, varying between ~0.10% and 0.90%. The average P_2O_5 content was 0.47%, 0.45% and 0.43% for MFP, DHP and TSP, respectively. Considering that the distance between two consecutive spots is 190 μm, that the spot diameter is 20 μm, and that no analysis has a P_2O_5 value of less than 0.10%, it is concluded that a better phosphate distribution (higher content) is obtained in the OPC paste with an admixture corrosion inhibitor procedure (Fig. 4), than with a migrating corrosion inhibitor procedure (Fig. 3), in which the average P_2O_5 content was ~0.10%.

Fig. 5 shows the corrosion potential (E_{corr}) versus time for steel bars embedded in mortar specimens immersed in the aqueous phosphate solutions (MFP, DHP or TSP) or distiled water (migrating corrosion inhibitor specimens). The E_{corr} values are situated at levels of low or medium risk of corrosion. Even so, the E_{corr} parameter can be used to define the probability of corrosion in the carbon steel embedded in OPC mortar: for $E_{corr} < -0.43$ V vs. SCE the probability of corrosion is high (~90%), for -0.43 V $< E_{corr} < -0.28$ V vs. SCE corrosion is uncertain, and for $E_{corr} > -0.28$ V vs. SCE there is a 10% probability of corrosion [31]. Only the experiment performed by immersion in distiled water presented a high risk of corrosion. It can be seen that the E_{corr} value for specimens immersed in the aqueous phosphate solutions is less negative (noble) that for the specimen immersed in distiled water (without inhibitor). Thus, E_{corr} values indicate that MFP, DHP and TSP may be considered anodic inhibitors. Specimens immersed in the aqueous DHP solution present the most noble corrosion behaviour, with the least negative E_{corr} value.

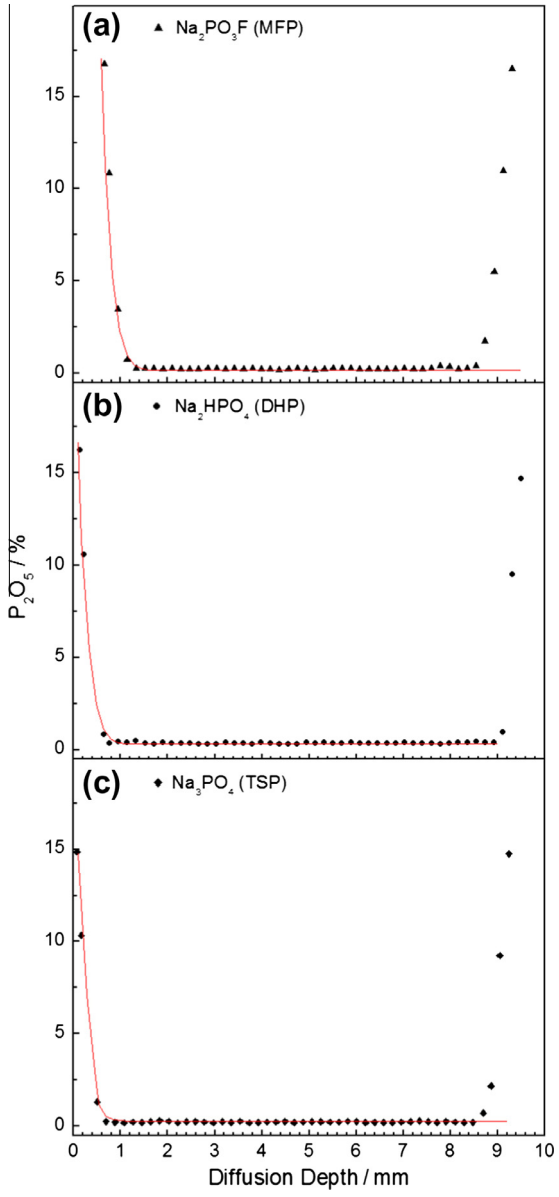

Fig. 3. Phosphorus content (as P_2O_5) versus diffusion depth (penetration) for migrating corrosion inhibitor specimens using Fick's law. 60 days Immersion in 0.2 M aqueous: (a) Na_2PO_3F (MFP) solution, (b) Na_2HPO_4 (DHP) solution, and (c) Na_3PO_4 (TSP) solution. To homogenise *y*-axis scale data, the first values of (a) were not included.

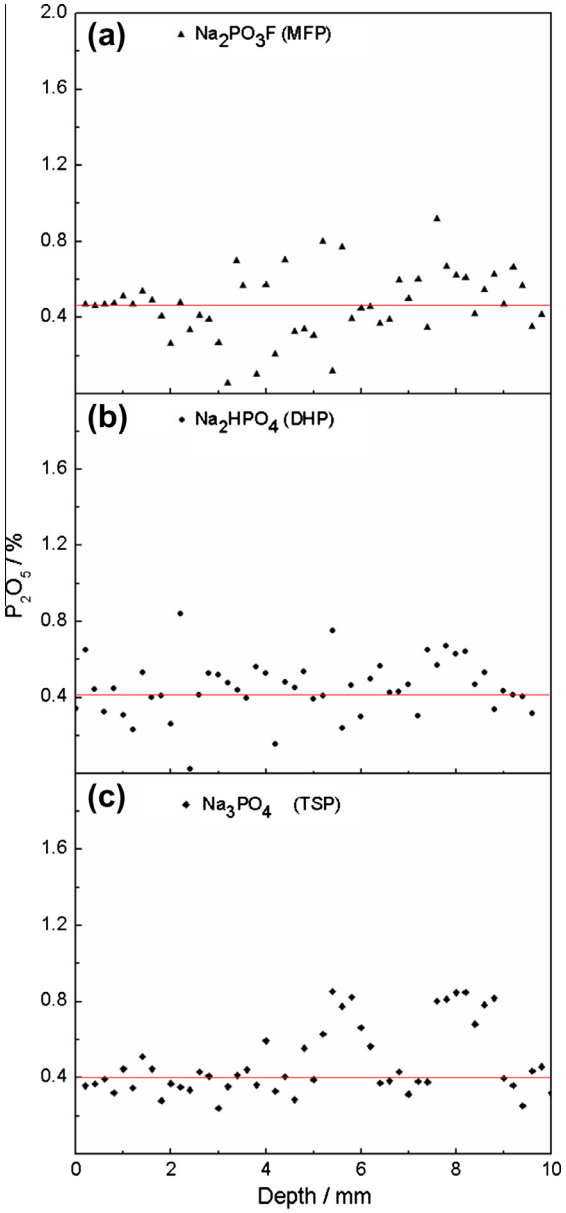

Fig. 4. Phosphorus content (as P_2O_5) versus depth (penetration) for admixture corrosion inhibitor specimens. Ordinary Portland cement mixed with 3%: (a) Na_2PO_3F (MFP), (b) Na_2HPO_4 (DHP), and (c) Na_3PO_4 (TSP).

Table 2
Penetration depth (μm) for migrating corrosion inhibitor specimens immersed for 60 days in aqueous Na_2PO_3F (MFP), Na_2HPO_4 (DHP) and Na_3PO_4 (TSP) solutions, determined as phosphorus (P_2O_5), and diffusion coefficient of anion.

Compound (Anion)	Penetration depth (μm) Phosphorus (P_2O_5)	Diffusion coefficient of anion ($cm^2\ s^{-1}$)
Na_2PO_3F (PO_3F^{2-}) (MFP)	1114	1.8×10^{-8}
Na_2HPO_4 (HPO_4^{2-}) (DHP)	380	6.7×10^{-9}
Na_3PO_4 (PO_4^{3-}) (TSP)	126	5.0×10^{-9}

Fig. 6 shows the corrosion current density (i_{corr}), estimated from R_p measurements, versus time for steel bars embedded in mortar specimens immersed in the aqueous phosphate solutions (MFP, DHP or TSP) or distiled water (migrating corrosion inhibitor specimens). The i_{corr} values are situated at levels of low or medium risk of corrosion. The dotted line indicates the approximate limit for passive steel values, $\leqslant 0.1\ \mu A\ cm^{-2}$ [32]. The best corrosion inhibitor behaviour is shown by the MFP and DHP compounds, with i_{corr} values of $<0.1\ \mu A\ cm^{-2}$, typical of the passive state. The TSP specimens are passive from 10 to 30 days, after which time the i_{corr} increases. The blank specimen (immersion in distiled water without inhibitor) was actively corroding.

Fig. 7 shows the corrosion potential (E_{corr}) versus time for steel bars embedded in mortar specimens prepared by mixing 3% of solid phosphate powder (MFP, DHP or TSP) with OPC, water and sand (admixture corrosion inhibitor specimens). The mortar specimens were stored in desiccators at saturation RH (~100%). As for the migrating corrosion inhibitor specimens (Fig. 5), the best corrosion inhibitor behaviour is shown by the DHP compound. The specimens with MFP and TSP compounds show E_{corr} values at the medium risk of corrosion level. From a practical point of view, Fig. 7 and also Fig. 5 present excellent results as the use of DHP or TSP is a good alternative to the expensive MFP compound.

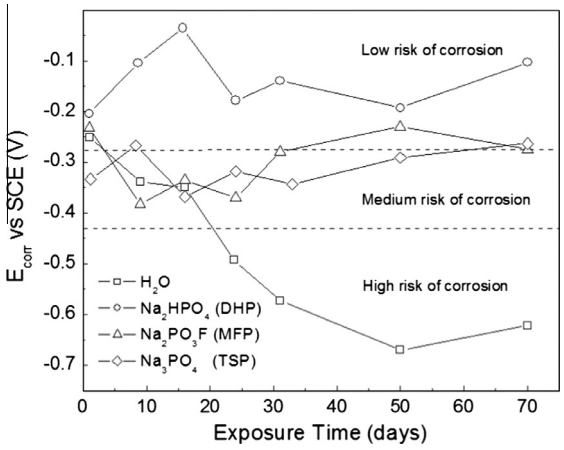

Fig. 5. Corrosion potential (E_{corr}) versus exposure time for migrating corrosion inhibitor specimens. Steel bars embedded in ordinary Portland cement (OPC) mortar and immersed in distiled water (H_2O) (blank experiment) or in 0.2 M aqueous phosphate, Na_2HPO_4 (DHP), Na_2PO_3F (MFP) or Na_3PO_4 (TSP) solution.

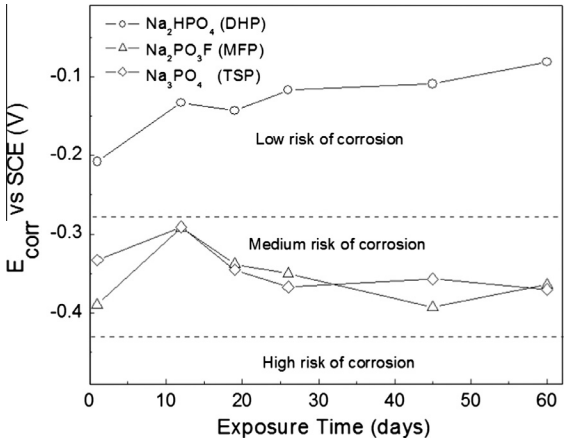

Fig. 7. Corrosion potential (E_{corr}) versus exposure time for admixture corrosion inhibitor specimens. Steel bars embedded in ordinary Portland cement (OPC) mixed with 3% Na_2HPO_4 (DHP), Na_2PO_3F (MFP) or Na_3PO_4 (TSP). The specimens were stored in desiccators at ~100% RH.

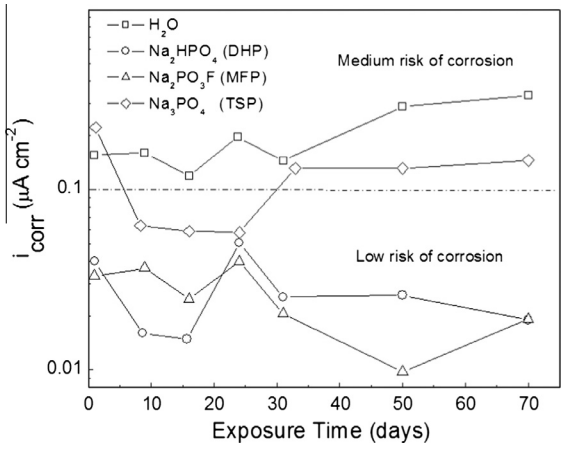

Fig. 6. Corrosion current density (i_{corr}), estimated from R_p measurements, versus exposure time for migrating corrosion inhibitor specimens. Steel bars embedded in ordinary Portland cement (OPC) mortar and immersed in distiled water (H_2O) (blank experiment) or in 0.2 M aqueous phosphate, Na_2HPO_4 (DHP), Na_2PO_3F (MFP) or Na_3PO_4 (TSP) solution.

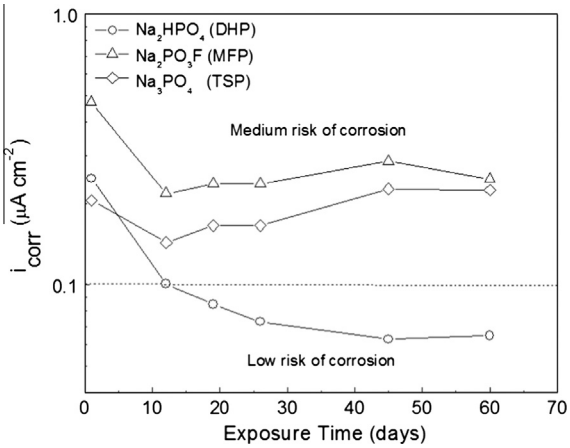

Fig. 8. Corrosion current density (i_{corr}), estimated from R_p measurements, versus exposure time for admixture corrosion inhibitor specimens. Steel bars embedded in ordinary Portland cement (OPC) mixed with 3% Na_2HPO_4 (DHP), Na_2PO_3F (MFP) or Na_3PO_4 (TSP). The specimens were stored in desiccators at ~100% RH.

Fig. 8 shows the corrosion current density (i_{corr}), estimated from R_p measurements, versus time for steel bars embedded in mortar admixture corrosion inhibitor specimens prepared by mixing 3% of solid phosphate powder (MFP, DHP or TSP) with OPC, water and sand. The mortar specimens were stored in desiccators at ~100% HR. The best corrosion inhibitor behaviour is shown by the DHP compound, with i_{corr} values situated at levels of low or medium risk of corrosion.

Fig. 9 shows the inhibitor efficiency (IE) versus time for steel bars embedded in mortar specimens immersed in the aqueous phosphate solutions (MFP, DHP or TSP) (migrating corrosion inhibitor specimens). The IE (%) value was obtained using the expression [33]:

$$IE(\%) = \frac{CR_{abs} - CR_{pre}}{CR_{abs}} \times 100 \quad (3)$$

where CR_{abs} and CR_{pre} are the steel corrosion rates estimated from R_p measurements in the absence and presence of inhibitor, respectively. In general, the best inhibition efficiency is shown by the MFP compound. Nevertheless, for 10 and 20 days experimentation the DHP compound showed the highest IE. In general, the order of inhibition efficiency is MFP > DHP > TSP.

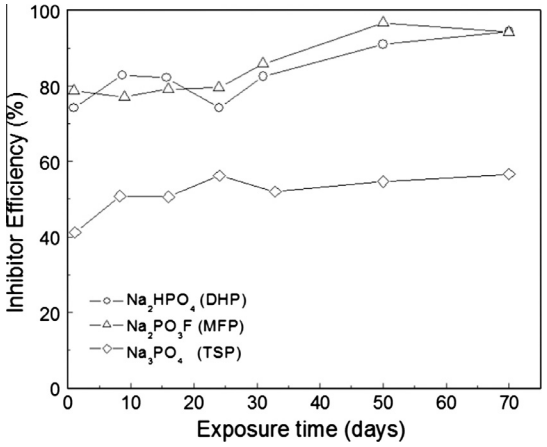

Fig. 9. Inhibitor efficiency (%) versus time for migrating corrosion inhibitor specimens. Steel bars embedded in ordinary Portland cement (OPC) mortar immersed in aqueous phosphate, Na_2HPO_4 (DHP), Na_2PO_3F (MFP) or Na_3PO_4 (TSP) solution.

4. Discussion

The low penetration of phosphate ions in the migrating corrosion inhibitor specimens (1114 μm, 380 μm and 126 μm for MFP, DHP and TSP, respectively) may be explained, on the one hand, by the very low porosity of the tested OPC paste, and on the other hand by the reaction of phosphate ions with portlandite in the OPC, yielding apatite which is precipitated in the pore network. The formation of apatite probably blocks any further inhibitor penetration.

Ormellese et al. [4], studying a tertiary amine with inorganic phosphorus compounds as a corrosion inhibitor for reinforcing steel, reported a capillary coefficient of $\sim 3\ g\ m^{-2}\ s^{-1/2}$ for the inhibitor and $\sim 6\ g\ m^{-2}\ s^{-1/2}$ for water, indicating that the inhibitor penetration was limited to the first 20 mm of concrete depth. This behaviour was associated to the high inhibitor viscosity compared to water and, above all, a chemophysical interaction between the inhibitor mixture and the concrete pore surface leading to the formation of precipitated compounds that block the concrete porosity. In view of these results, the lower penetration of the inhibitors tested in the present research (126–1114 μm) can probably be explained by the interaction between the inhibitor and the OPC paste.

According to Chaussadent et al. [34], the chemical reactions between the phosphate solution and the substrate (portlandite) are:

$$6Ca(OH)_2 + 3PO_3F^{2-} + 6Na^+ \leftrightarrows Ca_5(PO_4)_3F + CaF_2 + 6OH^- + 6Na^+ + 3H_2O \quad (4)$$

$$5Ca(OH)_2 + 3PO_4^{3-} + 9Na^+ \leftrightarrows Ca_5(PO_4)_3OH + 9OH^- + 9Na^+ \quad (5)$$

$$5Ca(OH)_2 + 3HPO_4^{2-} + 6Na^+ \leftrightarrows Ca_5(PO_4)_3OH + 6OH^- + 6Na^+ + 3H_2O \quad (6)$$

Using the standard free energy values (ΔG_f^0) reported by Wagman et al. [35], and Tacker and Stormer [36], for the different species, it was possible to calculate the equilibrium constants for Eqs. (4)–(6), which allow the following activities of phosphate ions in equilibrium with the interstitial solution to be calculated for the migrating corrosion inhibitor specimens: $\log a_{PO_3F^{2-}} = -23.02$, $\log a_{PO_4^{3-}} = -10.81$, and $\log a_{HPO_4^{2-}} = -11.16$. These activity values are very low and corroborate the low mobility of phosphate ions in the OPC paste. However, calcium fluorophosphate or calcium hydroxide phosphate may precipitate as amorphous phases which are more soluble than the crystalline phases and consequently have a higher activity and mobility phosphate ions. The extraordinarily low activity value calculated for monofluorophosphate ion indicates lower mobility than the PO_4^{3-} and HPO_4^{2-} ions. The discordance between this result and the diffusion process experiments (Table 2) may also be explained, according to Rowley and Stuckey [37], and Mehta and Simpson [38], by assuming that the reaction between portlandite and monofluorophosphate (PO_3F^{2-}) yields calcium monofluorophosphate dihydrate and subsequently, according to Ostwald's rule, changes to the most stable fluorapatite according to the following equilibriums [39]:

$$Ca(OH)_2 + PO_3F^{2-} + 2Na^+ + 2H_2O \leftrightarrows Ca(PO_3)F \cdot 2H_2O + 2OH^- + 2Na^+ \quad (7)$$

and

$$3Ca(OH)_2 + 3Ca(PO_3F) \cdot 2H_2O \leftrightarrows Ca_5(PO_4)_3F + CaF_2 + 9H_2O \quad (8)$$

Using the ΔG_f^0 for calcium monofluorophosphate dihydrate proposed by Duff [40]: $-2221.29\ kJ\ mol^{-1}$, the equilibrium constant of Eq. (7) and the activity of the monofluorophosphate ion were calculated, $\log a_{PO_3F^{2-}} = -4.66$. This value would explain the high diffusion of this ion in the OPC paste. Thus a precipitation-diffusion mechanism may be proposed. Precipitation of the $Ca(PO_3)F{\cdot}2H_2O$ phase takes place following an evolution to $Ca_5(PO_4)_3F$, with a drastic reduction in the activity of the interstitial PO_3F^{2-} ion.

Table 2 lists the effective diffusion coefficients (D) obtained using Eq. (2). The D values are $1.8 \times 10^{-8}\ cm^2\ s^{-1}$ for MFP, $6.7 \times 10^{-9}\ cm^2\ s^{-1}$ for DHP and $5.0 \times t10^{-9}\ cm^2\ s^{-1}$ for TSP. These results indicate a diffusion rate order of MFP > DHP > TSP. Phosphate diffusion is a time-dependent process that decreases with time since the capillary pore network will be altered as precipitation products continue to form. Furthermore, some phosphate ions will become chemically bound as they penetrate through the pore network and form precipitate phosphate compounds. Iron phosphate forms a thin film on both the surface and the core of the OPC paste because it is perfectly mixed with the remaining materials. This protects it from later attacks and also insulates the OPC paste from the aggressive environment, besides providing good adherence to the reinforcing steel bars.

E_{corr} results indicate that the presence of DHP, MFP or TSP had a positive influence on the inhibition of corrosion. The E_{corr} was shifted in the anodic direction (less negative) and the steel/OPC system was less prone to corrosion. E_{corr} values were situated at levels of low or medium risk of corrosion with both migrating corrosion inhibitor and admixture corrosion inhibitor specimens in the presence of phosphate compounds (Figs. 5 and 7, respectively). In contrast, the experiment involving immersion in distiled water without inhibitor (Fig. 5) presented a high risk of corrosion. Comparing the E_{corr} values for migrating corrosion inhibitor specimens in the presence and absence of inhibitor (Fig. 5), DHP, MFP or TSP may all be considered anodic inhibitors when acting as migrating corrosion inhibitors.

i_{corr} Values, estimated from R_p measurements, were situated at low or medium levels of corrosion risk, see Fig. 6 for migrating corrosion inhibitor specimens. The dotted line ($\leqslant 0.1\ \mu A\ cm^{-2}$) is the approximate limit for the passivity of steel [32]. The best corrosion inhibitor behaviour for migrating corrosion inhibitor specimens was shown by the MFP and DHP compounds. The specimens containing TSP compound were active at the start of the experiment, passivated between 10 and 30 days, and the i_{corr} increased to the active state (medium risk of corrosion) after 30 days, see Fig. 6. A medium risk of corrosion was shown by the migrating corrosion inhibitor specimens in the absence of inhibitor, i.e. immersed in distiled water. For the admixture corrosion inhibitor specimens (Fig. 8) the best corrosion inhibitor behaviour was shown by the DHP compound, which presented i_{corr} values in the passive state for most of the tested time.

i_{corr} Values (Figs. 6 and 8) indicate active corrosion at the start of the experiment followed by a drop in the corrosion current density which may be associated with the protection supplied by the inhibitor or by the surrounding alkaline medium of the pore network solution. After this initial time an increase in the i_{corr} was observed which may be explained by a precipitation-diffusion mechanism. Only in the presence of the DHP compound, for both migrating corrosion inhibitor and admixture corrosion inhibitor specimens, were the steel reinforcements in the passive state for all the experimental time tested. The MFP compound, which supplied passivity for the steel embedded in migrating corrosion inhibitor specimens (Fig. 6), came in second place. This result is interesting because it suggests that the conventional MFP compound could be replaced by the cheaper DHP.

The average P_2O_5 content was 0.47%, 0.45% and 0.43%, respectively, for MFP, DHP and TSP, in the case of admixture corrosion inhibitor specimens, and ~0.10% for all three phosphates in the case of migrating corrosion inhibitor specimens. This difference in the P_2O_5 content was probably not enough to bring about a change in corrosion inhibition behaviour, since the i_{corr} was of

the same order for migrating corrosion inhibitor specimens (Fig. 6) and admixture corrosion inhibitor specimens (Fig. 8).

It can therefore be said that the procedure based on a diffusion process, by immersion in an aqueous phosphate solution, is not the best approach. Preventing corrosion can be well solved by mixing the phosphate compound with the cement paste. This procedure is easy to apply, and a small amount of DHP, of the order of 1%, would probably be enough to protect the steel reinforcement while avoiding the interaction between DHP with calcium hydroxide (portlandite).

The DHP compound showed the highest inhibition efficiency (IE) for 10 and 20 days of experimentation using migrating corrosion inhibitor specimens. Nevertheless, in general the best IE was shown by the MFP compound. The order of IE was MFP > DHP > TSP. These results corroborate the fact that, from a practical point of view, DHP and TSP compounds are good alternatives to the expensive MFP compound for use as migrating corrosion inhibitors.

5. Conclusions

The average P_2O_5 content for specimens prepared with an admixture inhibitor process was 0.47%, 0.45% and 0.43% for MFP, DHP and TSP, respectively, and for specimens immersed in aqueous phosphate solutions (inhibition mechanism as a migrating corrosion inhibitor) the average P_2O_5 content was ~0.10% for all three phosphates. This difference is probably not enough to cause a change in corrosion inhibition behaviour, since the i_{corr} was of the same order for both types of specimens. Thus, the admixture or migrating corrosion inhibitor approaches were about equally effective in corrosion inhibition.

Phosphate diffusion is a time-dependent process, which decreases with time as the capillary pore network becomes altered by the continuing formation of precipitation products. Furthermore, some phosphate ions will become chemically bound as they penetrate the pore network and form precipitate phosphate compounds. The experimental results of the migrating corrosion inhibitor diffusion coefficient were used as the base to calculate the diffusion of MFP, DHP and TSP compounds through the OPC paste.

The three tested corrosion inhibitors (MFP, DHP or TSP) present good inhibition behaviour. The order of efficiency for phosphates acting as migrating corrosion inhibitors was MFP > DHP > TSP. The results indicate that DHP and TSP compounds are good alternatives to the expensive MFP compound. For admixture corrosion inhibitor specimens the best corrosion inhibitor behaviour was shown by the DHP compound, which presented i_{corr} values in the passive state for most of the tested time.

Acknowledgements

The authors express their gratitude to Project BIA2008-05398 of the CICYT, Spain, for financial support. D.M. Bastidas gratefully acknowledges funding from the Ramon & Cajal Program of the Spanish Ministry of Science and Innovation. M. Criado and S. Fajardo express their gratitude to the Spanish Research Council (CSIC) for their contracts through the JAE Program, co-financed by the European Social Fund.

References

[1] García J, Almeraya F, Barrios C, Gaona C, Núñez R, López I, et al. Effect of cathodic protection on steel–concrete bond strength using ion migration measurements. Cem Concr Compos 2012;34(2):242–7.
[2] Portanguen AD, Prince W, Lutz T, Arliguie G. Detection or quantitative analysis of a corrosion inhibitor, the sodium monofluorophosphate, in concrete. Cem Concr Compos 2005;27(6):679–87.
[3] Söylev TA, Richardson MG. Corrosion inhibitors for steel in concrete: state-of-the-art report. Constr Build Mater 2008;22(4):609–22.
[4] Ormellese M, Bolzoni F, Goidanich S, Pedeferri MP, Brenna A. Corrosion inhibitors in reinforced concrete structures. Part 3 migration of inhibitors into concrete. Corros Eng Sci Technol 2011;46(4):334–9.
[5] Hara M, Ichino R, Okido M, Wada N. Corrosion protection property of colloidal silicate fuln on galvanized steel. Surf Coat Technol 2003;169–170(2):679–81.
[6] Etteyeb N, Sánchez M, Dhouibi L, Alonso MC, Takenouti H, Triki E. Effectiveness of pretreatment method to hinder rebar corrosion in concrete. Corros Eng Sci Technol 2010;45(6):435–41.
[7] Singh DDN, Ghosh R. Molybdenum–phosphorus compounds based passivator to control corrosion of hot dip galvanized coated rebars exposed in simulated concrete pore solution. Surf Coat Technol 2008;202(19):4687–701.
[8] Robin JJ, Durand J, Cot L, Bonnel A, Duprat M, Dabosi F. Etude physicochimique et electrochimique de la protection d'un acier au carbone par les monofluorophosphates. I. Influence d'un traitement de conversion chimique. J Appl Electrochem 1982;12(6):701–10.
[9] Loqmane S, Laamari R, Derja A, Berraho M. Sinthèse et charactérisation de $ZnPO_3F{\cdot}5/2H_2O$ – evaluation des propriétés anticorrosion vis-à-vis de substrats de fer. Ann Chim Sci Mater 2000;25(2):127–41.
[10] Sankara-Narayanan TSN. Surface pretreatment by phosphate conversion coatings – a review. Rev Adv Mater Sci 2005;9(2):130–77.
[11] Rausch W. The phosphating of metals. London: Finishing Publications Ltd.; 1990.
[12] Grundmeier G, Rossenbeck B, Roschmann KJ, Ebbinghaus P, Stratmann M. Corrosion protection of Zn-phosphate containing water borne dispersion coatings. Part 2: Investigations of the corrosive de-adhesion of model latex coatings on iron. Corros Sci 2006;48(11):3716–30.
[13] Manna M. Characterisation of phosphate coatings obtained using nitric acid free phosphate solution on three steel substrates: an option to simulate TMT rebars surfaces. Surf Coat Technol 2009;203(13):1913–8.
[14] Manna M. Effect of steel substrate for phosphate treatment: an option to simulate TMT rebar surface. Corros Sci 2009;51(3):451–7.
[15] Jalili MM, Moradian S, Hosseinpour D. The use of inorganic conversion coatings to enhance the corrosion resistance of reinforcement and the bond strength at the rebar/concrete. Constr Build Mater 2009;23(1):233–8.
[16] Simescu F, Idrissi H. Corrosion behaviour in alkaline medium of zinc phosphate coated steel obtained by cathodic electrochemical treatment. Corros Sci 2009;51(4):833–40.
[17] Ngala VT, Page CL, Page MM. Corrosion inhibitor systems for remedial treatment of reinforced concrete. Part 2: sodium monofluorophosphate. Corros Sci 2003;45(7):1523–37.
[18] González JA, Ramírez E, Bautista A. Protection of steel embedded in chloride-containing concrete by means of inhibitors. Cem Concr Res 1998;28(4):577–89.
[19] Song H-W, Saraswathy V, Muralidharan S, Lee C-H, Thangavel K. Corrosion performance of steel in composite concrete system admixed with chloride and various alkaline nitrites. Corros Eng Sci Technol 2009;44(6):408–15.
[20] Bastidas DM, La Iglesia VM, Criado M, Fajardo S, La Iglesia A, Bastidas JM. A prediction study of hydroxyapatite entrapment ability in concrete. Constr Build Mater 2010;24(8):2646–9.
[21] Tritthart J. Transport of a surface-applied corrosion inhibitor in cement paste and concrete. Cem Concr Res 2003;33(6):829–34.
[22] Alonso C, Andrade C, Argiz C, Mairic B. Na_2PO_3F as inhibitor of corroding reinforcement in carbonated concrete. Cem Concr Res 1996;26(3):405–15.
[23] Mechmeche LB, Dhouibi L, Ben-Ouezdou M, Triki E, Zucchi F. Investigation of the early effectiveness of an amino-alcohol based corrosion inhibitor using simulated pore solutions and mortar specimens. Cem Concr Compos 2008;30(3):167–73.
[24] Söylev TA, McNally C, Richardson M. The effect of a new generation surface-applied organic inhibitor on concrete properties. Cem Concr Compos 2007;29(5):357–64.
[25] Wombacher F, Maeder U, Marazzani B. Aminoalcohol based mixed corrosion inhibitors. Cem Concr Compos 2004;26(3):209–16.
[26] López-Acevedo V, Viedma C, González V, La Iglesia A. Salt crystallization in porous construction materials. 2. Mass transport and crystallization. J. Cryst. Growth 1997;182(1–2):103–10.
[27] Stern M, Geary AL. Electrochemical polarization. I. A theoretical analysis of the shape of polarization curves. J Electrochem Soc 1957;104(1):56–63.
[28] Miranda JM, Fernández-Jiménez A, González JA, Palomo A. Corrosion resistance in activated fly ash mortars. Cem Concr Res 2005;35(6):1210–7.
[29] Bard AJ, Faulkner LR. Electrochemical methods fundamentals and applications. New York: Wiley; 1980. p. 144.
[30] Yu H, Hartt WH. Effects of reinforcement and coarse aggregates on chloride ingress into concrete and time-to-corrosion: Part 1 – spatial chloride distribution and implications. Corrosion 2007;63(9):843–9.
[31] ASTM C 876-99 Standard. Standard test method for half-cell potential of uncoated reinforcing steel in concrete. Annual book for ASTM Standards. Philadelphia: American Society for Testing and Materials; 1999.
[32] Andrade C, Alonso MC, González JA. An initial effort to use the corrosion measurements for estimating rebar durability. In: Burke NS, Chaker V, Whiting D, editors. Corrosion Rates of Steel in Concrete, STP 1065. Philadelphia: ASTM, American Society for Testing and Materials; 1990. p. 29.
[33] Criado M, Martínez-Ramírez S, Fajardo S, Gómez PP, Bastidas JM. Corrosion rate and corrosion product characterization using Raman spectroscopy for steel embedded in chloride-polluted fly ash mortar. Mater Corros 2013;64(5):372–80.
[34] Chaussadent T, Nobel-Pujol V, Farcas F, Mabille I, Fiaud C. Effectiveness conditions of sodium monofluorophosphate as a corrosion inhibitor for concrete reinforcements. Cem Concr Res 2006;36(3):556–61.

[35] Wagman DD, Evans WH, Parker VB, Schumm RH, Halow I, Bailey SM, Churney ICL, Nuttall RL. The NBS tables of chemical thermodynamic properties Selected values for inorganic and C-1 and C-2 organic-substances in SI units. J Phys Chem Ref Data 1982;11(Sup. 2):1–390.
[36] Tacker RC, Stormer Jr JC. A thermodynamic model for apatite solid solutions, applicable to high-temperature geologic problems. Am Min 1987;74(7–8):877–88.
[37] Rowley HH, Stuckey JE. Preparation and properties of calcium monofluorophosphate dihydrate. J Am Chem Soc 1956;78(17):4262–3.
[38] Mehta S, Simpson DR. Fluoride in apatite: substitution of monofluorophosphate for orthophosphate. Am Min 1975;60(1–2):134–8.
[39] Tavassoli Z, Sear RP. Homogeneous nucleation near a second phase transition and Ostwald's step rule. J Chem Phys 2002;116(12):5066–72.
[40] Duff EJ. The transformation: brushite–calcium monofluorophosphate under aqueous conditions. J Appl Chem Biotechnol 1972;22(4):475–81.